LA-12315-MS

Received by OSTI
JUL 1992

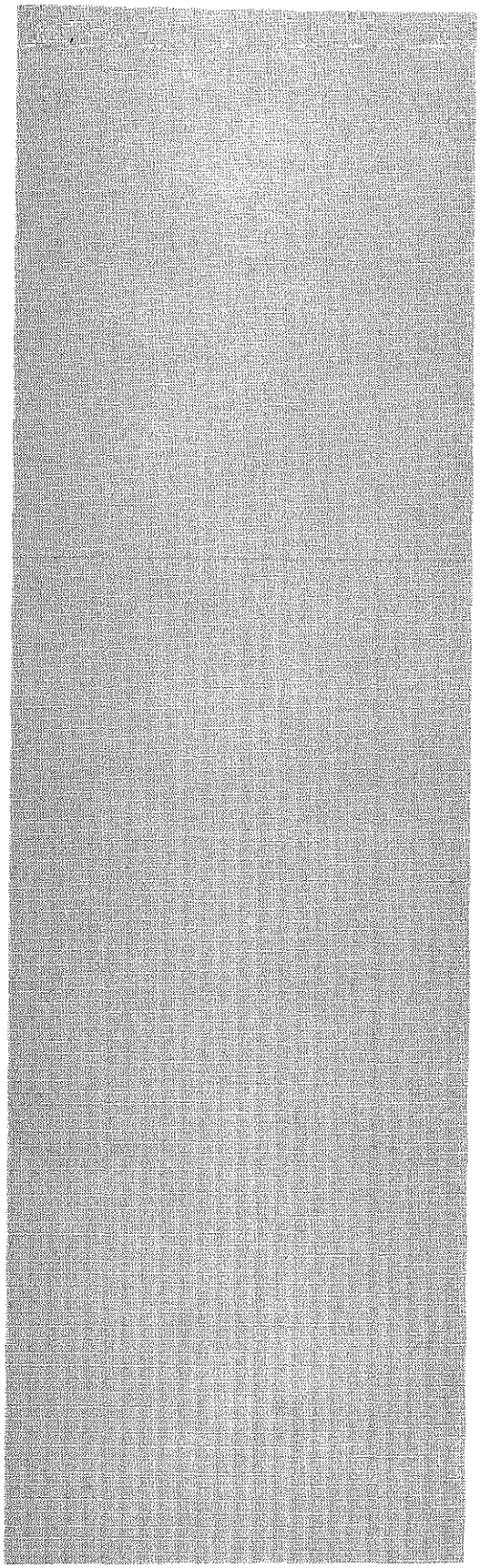

# *Evaluation of Source-Term Data for Plutonium Aerosolization*

Los Alamos

*Los Alamos National Laboratory is operated by the University of California for the United States Department of Energy under contract W-7405-ENG-36.*

DISTRIBUTION OF THIS DOCUMENT IS UNLIMITED

*An Affirmative Action/Equal Opportunity Employer*

*This report was prepared as an account of work sponsored by an agency of the United States Government. Neither The Regents of the University of California, the United States Government nor any agency thereof, nor any of their employees, makes any warranty, express or implied, or assumes any legal liability or responsibility for the accuracy, completeness, or usefulness of any information, apparatus, product, or process disclosed, or represents that its use would not infringe privately owned rights. Reference herein to any specific commercial product, process, or service by trade name, trademark, manufacturer, or otherwise, does not necessarily constitute or imply its endorsement, recommendation, or favoring by The Regents of the University of California, the United States Government, or any agency thereof. The views and opinions of authors expressed herein do not necessarily state or reflect those of The Regents of the University of California, the United States Government, or any agency thereof.*

LA--12315-MS

DE92 040908

# *Evaluation of Source-Term Data for Plutonium Aerosolization*

*John M. Haschke*

MASTER

Los Alamos National Laboratory
Los Alamos, New Mexico 87545

DISTRIBUTION OF THIS DOCUMENT IS UNLIMITED

# EVALUATION OF SOURCE-TERM DATA FOR PLUTONIUM AEROSOLIZATION

by

John M. Haschke

ABSTRACT

Relevant data are reviewed and evaluated in an effort to define the time dependence and maximum value of the source term for plutonium aerosolization during a fuel fire. The rate of plutonium oxidation at high temperatures is a major determinant of the time dependence. Analysis of temperature-time data for oxidation of plutonium shows that the rate is constant (0.2 g $PuO_2/cm^2$ of metal surface per min) and independent of temperature above 500°C. Total mass and particle distributions are derived for oxide products formed by reactions of plutonium metal and hydride. The mass distributions for products of all metal-gas reactions are remarkably similar with approximately 0.07 mass% of the oxide particles having geometric diameters $\leq$ 10 $\mu$m. In comparison, 25 mass% of the oxide formed by the $PuH_2+O_2$ reaction is in this range. Experimental values of mass fractions released during oxidation are evaluated and factors that alter the release fraction are discussed.

---

## INTRODUCTION

A broad spectrum of concerns are associated with the transportation of special nuclear materials. An accident scenario of interest is the possible dispersion of plutonium-containing particles into the environment if a shipping container for plutonium metal or a reactive plutonium compound is involved in a fuel fire. Reliable estimates of the hazards posed by such a plutonium release are contingent on the availability of technical data to define the source term for

aerosolization of plutonium oxide particles. Although several studies of plutonium aerosolization by burning metal are reported,[1-5] essential data are undefined. Information pertinent to plutonium release during self-sustained oxidation of plutonium has recently been reviewed and evaluated,[6] but the concerns addressed in that assessment differ significantly from those created by an external fire.

The aerosolization source term for the incident outline above varies during the course of the fire. The formation of aerosolizable particles from the non-aerosolizable metal is a complex process characterized by three distinct stages. The release probability and the source term are zero for a period of time during which the container temperature remains below the 640°C melting point of plutonium and the integrity of the container is preserved. The source term becomes non-zero when the container is breached by highly corrosive molten plutonium. Whereas most refractory metals such as Ti, V, Ta and W have limited solubilities in liquid plutonium[7] and are breached rather slowly, other metals such as steel readily form low-melting intermetallic phases[7] and are more rapidly breached. During this second stage, the source term increases with time as liquid metal progressively escapes from the container and reacts to form particles of plutonium oxide. The rates of these processes determine the length of time required to convert the metal to oxide, and the rate at which the source term increases from zero to a constant maximum value marked by complete oxidation. During the third stage the source term is invariant and defined by the total quantity of plutonium oxide and the aerosolizable fraction of that product. The maximum theoretical amount of oxide may not be dispersed because of kinetic limitations; the length of time to approach that point is very incident specific.

This report addresses important factors for defining the time dependence of the source-term and its maximum value for the scenario of interest. These factors are the oxidation kinetics of plutonium metal and plutonium hydride at

temperatures up to 1000°C, the particle distribution of products formed by those reactions and the kinetics of processes limiting entrainment of particles. Since some of the required information is divergent or unavailable, the conclusions of this report are based on a broad spectrum of literature describing fundamental and engineering studies and in certain cases rely on the use of interpolation, extrapolation and modeling.

## FUNDAMENTAL PROPERTIES

### Pertinent Physical and Chemical Properties

Plutonium is a reactive metal exhibiting complex properties and forming stable compounds with most other elements. The unalloyed metal has six allotropic forms between room temperature and its melting point at 640°C.[8] Differences in hardness and other properties are observed for each phase. Unalloyed plutonium, often described as "alpha phase," is a hard metal existing at room temperature. Since this form of Pu is only stable up to 122°C, the alpha phase is not actually present at the temperatures of interest. The delta phase is a malleable metal normally existing in the 315 to 457°C range, but this form occurs over a wide temperature range when plutonium is alloyed with gallium. The delta-phase alloy containing approximately 1 mass% Ga is stable when cooled to room temperature.

Plutonium forms two oxides, $Pu_2O_3$ and $PuO_2$. These friable crystalline phases are thermodynamically stable; their respective free energies of formation at 25°C are -378 and -238.5 kcal/mol.[9] $Pu_2O_3$, the lower-composition equilibrium product formed during oxidation of plutonium metal, is readily converted to $PuO_2$ in air. This conversion is so facile that only $PuO_2$ is observed on the surface of the metal under 500 torr $O_2$ at temperatures up to 500°C.[10]

Plutonium forms a complex series of hydrides in the composition range bounded by $PuH_2$ and $PuH_3$.[11] The cubic di-

hydride structure readily accommodates additional hydrogen, and a continuous solid solution forms between $PuH_2$ and $PuH_3$ as the temperature and hydrogen pressure are varied. The free energies of formation of $PuH_2$ and $PuH_3$ at 25°C are -31.2 and -40.4 kcal/mol, respectively. The hydrides are pyrophoric crystalline materials that react violently to form $PuO_2$ upon exposure to air.

The sizes of product particles formed by the $Pu+O_2$ and $Pu+H_2$ reactions are strongly dependent on the reaction temperature. Whereas all oxide particles formed at low temperature are 5 μm or less in size,[12] particles with diameters exceeding 3 mm are formed at temperatures above 500°C.[1] In a parallel way, the hydride obtained near room temperature is a fine powder and that formed at temperatures above 300°C contains centimeter-sized particles.[13] Possible origins of this temperature dependence are discussed in the next section.

## Oxidation Mechanisms

An understanding of the physical processes associated with oxidation of plutonium metal and hydride provides a basis for evaluating data relevant to source-term evaluation. The oxidation behavior of metal by air and oxygen is well defined and pertinent references are cited in recent reports.[10,14] Plutonium oxidation is a "paralinear" process involving three stages shown by the curve in Figure 1. If a clean metallic surface is exposed to oxygen, the extent of the ensuing reaction follows a functionality characteristic of a diffusion-controlled process. As the thickness of the adherent oxide layer increases on the metal surface, the rate of oxygen diffusion through that layer decreases according to a parabolic curve like that observed for stage I in Figure 1.

The formation of oxide particles begins during stage II. The second stage is characterized by a linear reaction extent-time curve with a slope that defines the constant oxidation rate. At the onset of stage II, the thickness of the adherent

product layer attains a critical value determined by the buildup of stress induced by forming low-density oxide (molar volume = 23.67 $cm^3/mol$) on the high-density metal (molar volume = 12.20 $cm^3/mol$). This stress is relieved by cracking and spalling of the oxide layer. Localized enhancement of the reaction rate occurs at spallation sites. As the oxide thickness increases at these reactive sites, the resulting decrease in rate is offset by spallation and rate enhancement at other sites. This process establishes a constant average layer thickness and a constant bulk reaction rate. Stage III is a similar linear process entered after a transition period, but the origin of this change is unknown.

Variations observed in the sizes of product particles from $Pu+O_2$ and other Pu+gas reactions with temperature are consistent with the spallation mechanism described above. The observed increase in particle size with increasing reaction temperature is interpreted as a combination of two factors. The first of these is variation of metal hardness and malleability with temperature. Hardness data for the allotropes of plutonium show a progressive decrease with each phase transition and a five-fold difference in the hardness value for alpha and delta phases.[15] The increasing malleability of plutonium with temperature reduces the stress generated at the product-metal interface and promotes formation of a thicker product layer before spallation occurs. Data for several actinide metal + hydrogen reactions indicate that formation of centimeter-sized hydride particles occurs if the reaction temperature equals or exceeds half the melting temperature of the metal in degrees centigrade.[13]

A second factor that may alter product particle size is kinetic in nature. Spallation of particles via a stress cracking process involves nucleation of cracks at the surface and propagation of those cracks through the stressed material with ultimate coalescence and formation of free particles. Nucleation and propagation are both time-dependent, and the time period available for their occurrence is important in

determining particle size. Although the temperature dependence of spallation is unknown, the activation energies are probably small compared to the $E_a$ of 33 kcal/mol for stage II oxidation.[10] Consequently, the growth rate of the oxide layer is large compared to the spallation rate at high temperatures and formation of large particles is favored. At room temperature the oxide growth rate is extremely slow and the longer time available for spallation favors extensive crack formation and small particle sizes. Since the activation energy for $Pu+H_2$ is low ($E_a$ = 2.0 kcal/mol)[13] and the hydriding rate at room temperature is $10^6$ times faster than the rate for $Pu+O_2$,[16] hydride products should contain larger particles than the oxide formed at the same temperature. Whereas the largest particle diameter observed for low-temperature hydride is near 100mm,[17] that for low-temperature oxide is approximately 5 $\mu$m.[12]

The oxidation of plutonium hydride is a secondary reaction for which little change in particle size is anticipated. The molar volume of $PuO_2$ is virtually identical to that for $PuH_2$ (23.17 $cm^3$/mol) and minimal stress should exist at the oxide-hydride interface. This rationale leads to the conclusion that the particle size distributions for the hydride reactant and oxide product should coincide. Experimental observations do not support this conclusion. The count mean diameter (1.5 $\mu$m) measured for the oxide product of the $PuH_2+O_2$ reaction[18] is noticeably shifted relative the mean value (5.0 $\mu$m) for the hydride[17] and the BET (Brunauer, Emmett, Teller) surface area of the sample increases by a factor of 3 to 5 during oxidation.[19]

The spallation mechanism occurring during hydride oxidation apparently involves a physical process other than interface stress produced by reactant-product mismatch. The observed decrease in particle size is consistent with a conceptual fracture mechanism based on fundamental properties of oxide and hydride. During oxidation, the thermodynamically stable chemical arrangement does not involve release of

gaseous hydrogen, but its adsorption to form a higher-stoichiometry hydride within the $PuH_2$-$PuH_3$ solid-solution region of the phase diagram.[11] As the $PuO_2$ layer forms on the surface of a particle, the product hydrogen dissolves in the residual hydride center of the particle. This process continues until the stoichiometry of the hydride core approaches the $PuH_3$ limit. Additional hydrogen cannot be absorbed or readily escape through the thick oxide layer. The resulting increase in internal pressure leads to particle fragmentation.

## Oxidation Kinetics

The oxidation of plutonium proceeds through several stages, but all of them do not have equal impact on the source term. As shown in Figure 1, completion of the parabolic process and onset of spallation occurs after 3 h at 300°C and 1 torr oxygen pressure. The time span of stage I decreases with increasing temperature and oxygen pressure and is not a major factor in determining the onset of particle spallation at temperatures above 640°C and at the 160 torr $O_2$ partial pressure of the atmosphere. Consequently, only stages II and III need be considered for establishing the time dependence of the source term.

The anticipated kinetic behavior of the $Pu+O_2$ reaction at temperatures of interest is shown by Arrhenius curves in Figure 2. Solid segments of the curves show the oxidation rate, K, in mg $O_2/cm^2$min measured for stages II and III at 500 torr $O_2$ pressure and temperatures up to 450°C.[10] Extrapolations of the temperature trends established by the data are shown by the dashed segments. The changes in slope correspond to transitions from low-temperature processes having activation energies of 19 kcal/mol to high-temperature processes having higher $E_a$ values of 33 and 46 kcal/mol for stages II and III, respectively. As shown by Figure 1, the transition from stage II to stage III occurs after an extended time period and the later stage may not be entered during the

time frame of a fire. K is also dependent on the $O_2$ pressure, P, and varies as $P^n$. Below 400°C, K is rather insensitive to P with $0 \leq n \leq 1/3$. Above 400°C, $n = 1/2$ for stage II and $n = 1$ for stage III.

The extrapolated rate curves in Figure 2 provide a basis for predicting oxidation rates for $Pu+O_2$ in air at elevated temperatures. Even for $n = 1$, the pressure correction from 500 to 160 torr $O_2$ reduces K by approximately a factor of two and is considered negligible. For stage II, a 40 s time period is calculated for completely oxidizing a 1 kg Pu sphere in air at 1000°C, and half of a 200 g Pu cylinder should react in about 30 s at 850°C. This prediction stands in sharp conflict with an experimental observation by Stewart showing that 115 g of a 200 g cylindrical sample remained unreacted after 23 min in a fuel fire at 860°C.[1] Possible origins of this discrepancy include: (a) error in the experimental observation (b) depletion of the oxygen concentration in the fuel fire atmosphere near the sample and (c) a change in oxidation mechanism that invalidates the Arrhenius extrapolation.

The validity of the experimental observation is seen by comparing oxidation rates derived from data reported by Stewart[1] with values obtained from similar data reported by Mishima.[3] Relevant data extracted from time-temperature curves are presented in Table I with average oxidation rates calculated for each test. The results obtained from Stewart's data are shown by solid symbols in Figure 2 and those from Mishima's data are shown by open symbols. Error limits in the rate are based on estimated uncertainties in reaction times and sample surface areas. Three significant results are evident: (a) the oxidation rates are in agreement, but slower than predicted by Arrhenius extrapolation, (b) the rates are independent of temperature in the range above 500°C and (c) the rates for unalloyed metal and gallium-containing alloy are indistinguishable. Although oxidation rates measured for various Ga-containing alloys in air at room temperature are a

factor of 10 to 100 less than that for unalloyed plutonium,[20] the oxidation rates of these metals appear to converge at a temperature near 500°C.[21] The average oxidation rate for plutonium at temperatures above 500°C is 0.16±0.08 g $PuO_2/cm^2min$.

The rate results provide insight into the potential effects of oxygen depletion during a fuel fire. Use of the square-root pressure dependence for the stage II rate shows that the $O_2$ pressure at the sample must be reduced to about 0.5 torr in order to produce the apparent reduction in rate at 860°C. Not only does this pressure seem inordinately low and improbable, but the possibility of kinetic control by oxygen depletion is virtually precluded by the other set of kinetic results. The oxidation rates for reaction in a fuel fire[1] are identical to those for self-sustained burning in flowing air that provided a twenty-five-fold excess of $O_2$.[3]

The existence of reducing conditions in a fuel fire merits further evaluation. Volatilization and cracking of hydrocarbons produce a non-oxidizing atmosphere. However, a significant fraction of the fuel must also burn in order to maintain a 1000°C flame temperature. High concentrations of $H_2O$, $CO_2$ and CO must be present in the fire. Reactions of these species with plutonium are thermodynamically favored and are expected to occur at the temperature of the flame. For example, the reported[22] oxidation rate of delta-stabilized plutonium by water vapor at 15 torr pressure and 500°C equals that for alloy oxidation by $O_2$ at 500 torr and 500°C.[10]

Although a definitive explanation is not possible for the rate behavior of $Pu+O_2$ above 500°C, a change in reaction mechanism provides the most reasonable interpretation. Three possibilities merit consideration. The first involves formation of a progressively thicker oxide layer on the metal with increasing temperature. This explanation is unlikely because the thickness increase must precisely compensate for the temperature-driven increase in transport rate across the layer. A particle size increase with temperature is not

evident above 500°C. An alternate possibility is the self-limiting nature of autothermic chemical reactions.[23] A limit on the rate of a self-sustaining reaction arises because thermal acceleration ceases when the point is reached where the rate of heat loss balances the rate of heat production. Since the sample temperature cannot increase beyond this point, a limiting condition and a constant rate are achieved. Further evaluation of this concept is needed to determine if autothermic control is operative. The most likely explanation for the constant rate is a gas phase transport limitation occurring for gas mixtures. Removal of oxygen from the gas at the gas-solid interface produces a layer of nitrogen and other unreactive gases at the surface. The oxidation rate is controlled by the transport of oxygen or oxygenated species across that layer.

A constant oxidation rate for plutonium at temperatures above 500°C is unexpected and inconsistent with conclusions described in a recent review.[6] According to earlier interpretations of experimental data, the rate of $Pu+O_2$ at high temperatures is altered by metal type, sample mass and temperature, but the data in Table I do not support these conclusions. The recommended burn rate of 180 g/h for plutonium does not recognize the well-established dependence of rate on the surface area of metal,[10,20] and cannot be reconciled with the observed oxidation of a 1.8 kg Pu sample in 55 min.[3] The value cannot be compared with the 0.2 g $PuO_2/cm^2min$ rate derived in this work or applied to a specific situation. Although the mathematics of source term calculation during the time-dependent period is simplified by the existence of a constant oxidation rate, definition of the oxide quantity present at a given point in time is complicated by lack of information about metal release rates and geometries of molten metal deposits formed during failure of containment vessels.

The oxidation of high-surface-area plutonium hydride is a two-stage process.[19] The initial stage is extremely rapid

with a negative activation energy ($E_a$ = -2.1 kcal/mol) suggesting that the oxidation rate is determined by the adsorption of $O_2$ on the surface. During this stage a diffusion barrier of oxide advances toward the centers of the hydride particles and leads to a comparatively slow second stage of reaction. This is a constant-rate process over time and has $E_a$ = 10.0 kcal/mol. Incomplete oxidation is observed at low temperatures in experiments conducted over the 50 to 360°C range at 10 torr $O_2$ pressure.

The kinetics of $PuH_2$+$O_2$ are altered by several factors. Increasing the reaction temperature dramatically increases the fraction of hydride consumed during the initial processes. Whereas only 20% of the hydride reacts in the initial rapid stage at 100°C, the hydride is totally oxidized via this process at temperatures above 400°C. At 10 torr $O_2$ pressure the first stage is complete within minutes.[19] The pyrophoric nature of the hydride powder formed at temperatures below 100°C is well documented and different from that of the coarse product obtained at temperatures above 300°C.[24] The low-temperature hydride ignites and burns spontaneously when exposed to air; the high-temperature product only ignites in air when heated to 270°C. Rapid and complete oxidation of either product is expected if a hydride container is breached and the shipment is exposed to a fuel fire.

## SIZE DISTRIBUTIONS

### Size Distribution Data for the Product of Pu+$O_2$

Size distribution data for the product of metal oxidation are essential for source term definition. Although particle size measurements are described by various workers, distributions are only reported for selected fractions, not for an entire oxide product. Whereas the particle size distributions of products from Pu+gas reactions are strongly temperature dependent up to 500°C, data for products obtained above 500°C suggest that thermal effects on size are minimal.

Derivation of a total distribution for high-temperature oxide necessitates the combination of size distributions for large and small particles. This combination process is accomplished using distribution data for products of other Pu+gas reactions to correlate separate distributions of oxide particles.

Cumulative mass distributions for large particle fractions formed by high temperature oxidation are reported by Stewart[1] and by Mishima.[2] The log-normal distributions of geometric particle diameters measured by Stewart for the fractions not entrained by the up-draft in fuel fire experiments are shown in Figure 3. Data for the residue obtained at 860°C (solid circles) are in good agreement with those for a 500°C product (open circles), but only the second distribution accounts for the entire oxide mass. As shown by solid triangles, a partial distribution[2] of an unentrained oxide residue formed by combustion in flowing air at temperatures up to 560°C is in good agreement with those for fuel-fire tests.

The curve defined by solid symbols in Figure 4 shows the cumulative particle distribution measured by Mishima[3] for an oxide fraction entrained by an air flow of 5.25 m/sec (11.7 mph). The sample was collected during self-sustained combustion of a 1.8 kg metal sample at 925°C. The data provide a uniquely detailed picture of particle dimensions in the micron and submicron size range, but their contribution to the total distribution of oxide particles is unknown.

Essential information for deriving a total distribution for the oxide is obtained by evaluating particle size data reported for products formed by reactions of plutonium with other gases. The cumulative particle distribution for plutonium hydride is derived from a distribution for powdered plutonium metal.[17] The metal was initially prepared by hydriding massive plutonium at room temperature and then thermally decomposing the hydride in vacuum to regenerate the metal.[13] Since the BET surface areas of the hydride and metal powders are identical and invariant after repeated hydride-

dehydride cycles, the geometric particle size distribution measured for the metal is adopted for the hydride. The cumulative particle size data obtained from the distribution presented by Stakebake[17] are listed in Table II with size-mass fraction data calculated for spherical particles with the stated geometric diameters. The resulting cumulative mass distribution for the hydride is shown by open triangles in Figure 3. A renormalized cumulative particle distribution for hydride sizes less than 10 $\mu$m is shown by open circles in Figure 4.

Several aspects of the size distributions in Figure 3 are important in defining a total distribution for plutonium oxide. Key features of the curves are their shapes and their regions of coincidence. The total mass distributions for oxide and hydride are defined by two linear segments implying bimodel distributions of particles in both products. Whereas the dimensions of the largest oxide particles are about 1 mm, the largest hydride particles are about 0.1 mm in size. This difference in large particle sizes contrasts sharply with the remarkably close agreement observed for all distributions in the size range below 50 $\mu$m. These features appear to be characteristic of the distributions for products of all Pu+gas reactions, not a fortuitous coincidence. Small particles with similar sizes might be formed during spallation processes that produce dissimilar large particles. Regardless of the basis for this coincidence, it suggests that distribution data for the hydride might be used as a guide for reconstructing a total distribution for high-temperature oxide formed by $Pu+O_2$.

Additional insight is gained from a parallel examination of the particle distributions in Figure 4. Although the resolution of particle fractions is much less for hydride than for oxide, the agreement observed between the curves suggests that the coincidence of particle sizes beginning near 50 $\mu$m is maintained into the submicron range. The count mean diameter (1.3 $\mu$m) for hydride particles $\leq$ 10 $\mu$m is in close agreement with that (1.2 $\mu$m) for the entrained oxide. The small

difference appearing at the upper end of the distribution may occur because the tubular collection apparatus used by Mishima[3] for sampling the airborne fraction tends to exclude particles with large diameters.[25] The observed coincidence of distributions suggests that hydride data can be substituted for oxide data in the small particle range.

Derivation of a meaningful total mass distribution for plutonium oxide requires that the distribution for large and small particles be combined without skewing the result. A reasonable approach is suggested by examining the mass distributions data for hydride in Table II and that for oxide in Figure 3. A small fraction (0.2%) of the hydride mass appears in the 15 $\mu$m cumulative fraction and 1.8% of the mass is included in the 30 $\mu$m cumulative fraction. A comparable amount (1.2%) of the mass is included in the 32 $\mu$m fraction of oxide residue. The two distributions may be combined by substituting the 30 $\mu$m cumulative mass fraction of hydride for the 32 $\mu$m cumulative mass fraction of the oxide.

The total mass distribution derived for high-temperature $PuO_2$ by the substitution method is presented in Table III and Figure 5. Comparison of the total distribution with the partial distribution in Figure 3 shows that all features of the oxide data are reproduced by the composite curve. Greater detail in the definition of small particle sizes is achieved by redistributing the 1.5 $\mu$m fraction for the hydride in accordance with Mishima's data in Figure 4. The accompanying particle distribution in Table III is based on a spherical particle assumption.

## Size Distribution Data for the Product of $PuH_2$+$O_2$

Size distributions of oxide particles produced by oxidation of plutonium hydride are described in studies by Edison et al.[4,5] and by Stakebake and Robinson.[18] Using the results of an extensive investigation of several Pu+gas reactions involving air, a mixture of gases designed to simulate combustion products of organics, $H_2$, an $H_2$+$N_2$ mixture

and $H_2$ followed by air exposure, Edison et al. conclude that the respirable particle fraction produced by exposing hydride to air is not significantly different from the fractions produced by other Pu+gas reactions. In earlier work, Stakebake and Robinson observed that oxidation of the hydride by air is accompanied by substantial particle size changes and by an increase in surface area.[18] This behavior is consistent with the pyrophoric nature of the hydride and the results reported by Stakebake and Robinson are selected as the basis for defining the size distribution of oxide formed from hydride.

The particle size distribution measured by Stakebake and Robinson[18] for the $PuH_2$+$O_2$ product is shown by the open symbols in Figure 6. Although 95% of the particles are included in the 8 $\mu$m cumulative fraction, the distribution of larger particles is undefined. As evidenced by comparing typical mass and particle distributions in Tables II and III, a substantial fraction of the mass usually resides in the largest 5% of the particles. The particle distribution given in Table IV is obtained by assuming that the linear log-normal particle distribution applies to particle sizes in excess of 8 $\mu$m. The accompanying mass distribution in Table IV is derived using a spherical particle assumption. The log-normal mass distribution defined by these data is shown by open symbols in Figure 7.

## Size Distribution Modeling of Secondary Products

Extrapolation of the particle distribution for the Pu+$O_2$ product beyond the 95% cumulative fraction seems insignificant, but the potential impact on the mass distribution is substantial. The largest 5% of the particles accounts for 80% of the oxide mass. The derived mass distribution is strongly dependent on extrapolated data and the second linear segment suggesting a bimodal mass distribution (cf. Figure 7) is based solely on extrapolation. A model for describing the fragmentation of reactant particles

during a secondary reaction like $PuH_2+O_2$ is developed in an effort to independently predict the product size distribution.

In concept, the fracture model applies a fixed fragmentation pattern to reactant particles having a known distribution and constructs a new distribution for the product. The basic assumption for defining the fragmentation pattern is that each spherical reactant particle with diameter d fractures to form new spherical particles. As shown by a two-dimensional section through a reactant sphere in Figure 8, the fragmentation pattern is defined by a closest-packed planar array of spheres with diameters $d_1$, $d_2$, and $d_3$ having magnitudes of 0.33 d, 0.13 d, and 0.05 d, respectively. The reactant sphere is approximated by adding an identical layer above and another below the initial array and by filling peripheral recesses on the upper and lower surfaces with $d_2$ spheres. Each reactant sphere produces 21 $d_1$ spheres, 30 $d_2$ spheres and 18 $d_3$ spheres. Since this composite array fills only 82% of the original sphere volume, the residual volume is distributed proportionally among the three fractions such that 91.65% of the volume or mass of the original sphere appears as $d_1$ spheres, 8.12% appears as $d_2$ spheres and 0.23% appears as $d_3$ spheres. Each individual mass fraction in the reactant distribution is reassigned according to these percentages. The new mass distribution is generated by categorizing and summing the product masses in appropriate fractions.

Mass and particle distributions derived for the $PuH_2+O_2$ product using the fracture model are presented in Table V. These results are based on the size distribution for $PuH_2$ in Table II after the 1.5 $\mu$m fraction was repartitioned to define a 0.5 $\mu$m fraction containing a mass fraction of $3.0X10^{-9}$. The fracture model was applied to hydride particles with sizes $\geq$ 15 $\mu$m. Masses of particles with sizes $\leq$ 8 $\mu$m were combined with those of new fragments to generate the mass distribution in Table V. The corresponding particle distribution is based on spherical particle assumption.



Next Section